A R C H I V E S O F M E T A L L U R G Y A N D M A T E R I A L S
Volume 57 2012 Issue 2
DOI: 10.2478/v10172-012-0048-x

E. CEVIK*, Y. SUN*, H. AHLATCI*

EFFECT OF PEAK-AGED HEAT TREATMENT ON CORROSION BEHAVIOR OF THE AA6063 ALLOY CONTAINING Al_3Ti

WPŁYW OBRÓBKI CIEPLNEJ NA KOROZJĘ STOPÓW AA6063 ZAWIERAJĄCYCH Al_3Ti

The purpose of this study is to analyse the microstructure and corrosion properties of homogenised and aged AA 6063 aluminium alloys, containing up to 2% Ti, after the conventional casting technique. The microstructure of the homogenised and aged alloys was examined using an optic microscope, and scanning electron microscope. The micro-hardness test was used for the hardness measurements of the investigated alloys. Corrosion tests were performed by suspending samples of certain sizes into 30 gr/l NaCl + 10 ml/l HCl solutions, measuring the mass loss; potentiodynamic polarisation measurements were carried out in the same solution. The microstructure characterization of the investigated alloys shows the Al (matrix), non-shaped dark globular grey-coloured phase and rod-shaped phases formed at the grain boundaries. The non-shaped dark grey-coloured phase is Mg_2Si. The rod-shaped phase, formed in the microstructure of the Ti-added AA 6063 alloys, is Al_3Ti. The Ti content of the alloy increases, the Al_3Ti phase tends to elongate and become plated. The results of the corrosion tests proved that the corrosion rate decreased in alloys containing less than 1% Ti, and the rate of corrosion increased in alloys containing more than 1% Ti, regardless of whether the alloys were homogenised and aged. Another observation was that aging heat treatment improved corrosion resistance.

Keywords: non ferrous metals and alloys, casting, corrosion, micro structure

Celem niniejszej pracy jest analiza mikrostruktury i właściwości korozyjnych poddanych obróbce cieplnej stopów aluminium AA 6063, zawierających do 2% Ti, po odlewaniu konwencjonalnym. Mikrostrukturę homogenizowanych stopów zbadano za pomocą mikroskopii optycznej i skaningowej mikroskopii elektronowej. Test mikrotwardości zastosowano do pomiaru twardości badanych stopów. Badania korozyjne przeprowadzono poprzez zawieszenie próbki o określonych rozmiarach w roztworze 30 gr/l NaCl + 10 ml/l HCl i pomiar ubytku masy; pomiary potencjo-dynamicznej polaryzacji zostały przeprowadzone w tym samym roztworze. Charakterystyka mikrostruktury badanych stopów pokazuje matrycę Al; ciemnoszare, nieregularne wydzielenia fazy Mg_2Si; oraz na granicach ziaren pręcikowe wydzielenia fazy Al_3Ti, obecne w mikrostrukturze stopów AA 6063 z dodatkiem Ti. Ze wzrostem zawartości Ti, wydzielenia fazy Al_3Ti stają się wydłużone i płytkowe. Wyniki testów korozyjnych wykazały, że szybkość korozji spadła w stopach zawierających mniej niż 1% Ti, a wzrosła w stopach zawierających więcej niż 1% Ti, niezależnie od tego, czy stopy były homogenizowane i starzone. Zaobserwowano, że obróbka cieplna podwyższa odporność stopów na korozję.

1. Introduction

Aluminium and its alloys are used in many fields, whether in daily life or industrially. The reasons why aluminium and its alloys are common use is because they have low density, they are easy to work with, they have high electrical conductivity, and they have high heat conductivity. However, aside from the advantages listed above, the engineering applications for aluminium and alloys are limited due to poor surface properties, and low abrasion resistance [1].

For many commercial Al alloys, the desirable mechanical properties are developed by adding alloys and applying heat treatment to heterogeneous microstructures. It is possible that adding alloying elements affects the wear properties of Al-Si-Mg, as it strengthens them through solid solution and hardening precipitation [2,3]. Ce, Cu, Cr, Fe, Mn, Ti, Zn, and Zr are some of the alloying elements that are added to these alloys. The added alloying elements either dissolve or form compounds within the microstructure.

Over the years, a number of studies have been carried out to assess the effect specific intermetallic particles and individual alloying additions have on corrosion damage in Al alloys, which arises from pitting and inter-granular type corrosion [4-15]. In situations where

* KARABUK UNIVERSITY, ENGINEERING FACULTY, METALLURGICAL AND MATERIALS ENGINEERING, 78050 KARABUK, TURKEY

the corrosion characteristics of constituent intermetallics have been rigorously characterised, intermetallics have been found to exhibit a complex behaviour such as active and/or noble. Until now the intermetallics confirmed to exist within Al alloys are [4-6,8,10-14]: Mg_2Si, $MgZn_2$, $Al_{20}Cu_2Mn_3$, $Al_{12}Mn_3Si$, Al_7Cu_2Fe, Al_2Cu, Al_2CuMg, Al_3Fe, $Al_{12}Mg_2Cr$, $Al_{20}Cu_2Mn_3$, Al_6Mn, Al_3Ti, Al_3Zr, Mg_2Al_3, and $Al_{32}Zn_{49}$.

The role of these intermetallics, excluding Mg_2Si and Al_3Ti, with respect to mechanical and corrosion properties, is beyond the scope of this paper; however, intermetallic particles in Al alloys can be classified in three main groups: precipitates ($MgZn_2$, Mg_2Al_3, Mg_2Si, Al_2Cu), constituent particles (Al_3Fe, Al_7Cu_2Fe, AlFe-Si and other AlFe particles), and dispersoids (Al_3Ti, A_6Mn, $Al_{20}Cu_2Mn_3$ and Al_3Zr). The sizes of precipitates range from Angstroms to fractions of a micrometer; formed by nucleation and growth in a supersaturated solid solution during natural or low temperature artificial aging. When precipitates are homogenously dispersed, their effect on localised corrosion behaviour is difficult to discern. However, when they are on or along the grain boundaries, they may affect inter-granular corrosion [5-7,9,14,15]. Constituent particles are comparatively large in size and range over a few tenths of a micrometer up to 10 micrometers. These particles may form during solidification, and are not appreciably dissolved during subsequent thermo-mechanical processing. Dispersoids are small particles that comprise alloying elements that are highly insoluble in Al alloys. These particles form at high temperatures and are present to control the grain size and re-crystallisation behaviour. Both constituent particles and dispersoids are susceptible to pitting corrosion because of their galvanic interaction with the Al matrix [7-9,13].

In a study conducted by Birbilis and Buchheit [11,12], they classified the intermetallics formed in Al alloys, based on them being active or passive, their corrosion potentials, and their corrosion current. In conclusion they proved that Al_3Ti and $Al_{20}Cu_2Mn_3$ had the lowest corrosion rate, while Mg_2Si and $MgZn_2$ had the highest corrosion rate.

Al-based intermetallics, especially Al_3Ti, are attracting interest because of their excellent properties. The combination of light weight and high strength makes Ti containing alloys very attractive for the aerospace and the automotive industry [16]. However, studies on the corrosion behaviour of the alloys containing the Al_3Ti intermetallic are limited.

The purpose of this study is to analyse the effects of adding Ti and applying aging heat treatment on the microstructure and corrosion properties of AA 6063 alloys.

2. Experimental Procedures

In this study, the pure Ti and AA6063 alloy, whose nominal chemical compound is Al – 0.5 Mg – 0.2 Fe – 0.4 Si, was used as starting materials. The AA 6063 quality ingot alloy was subject to a re-melting process, in order to add 1% or 2% Ti. During the re-melting process, applied at 750°C, in an electric-resistant melting furnace, with a 1200°C temperature capacity, the gassing process was applied by adding 0.4% of weight of C_6Cl_6 to the liquid alloy. The prepared melt was then poured into a permanent mould, heated to 300°C, with a mould cavity 50 mm in diameter and 250 mm in length. Homogenising and then aging heat treatment were carried out on the investigated casting alloys respectively.

The homogenising heat treatment for the investigated cast alloys was carried out by cooling the samples in the furnace, after keeping them at 500°C for 2 hours. Aging heat treatment, applied to the homogenised samples, was carried out by quenching, after keeping them at 500°C for two hours, and then the aging stages were applied at four hour intervals up to 48 hours, at 150°C. Both the homogenised and aged samples were subject to the hardness measurement test, microstructure characterisation, and corrosion test.

After preparing the samples in accordance with the standard metallographic procedure, the microstructures of the investigated alloys were analysed using a Leica DM ILM metallurgical optic microscope, a Leica DFC290 camera system, and a Jeol 6060 SEM (Scanning Electron Microscope) equipped with EDS (energy dispersive X-ray spectroscopy). EDS analysis was carried out on the light and grey-coloured regions of the microstructural images obtained during SEM assessment.

The hardness of the samples, prepared using the metallographic process, was measured using the Shimadzu HMV2 microhardness test device, by applying a 200-g sink load, and a Vickers indenter. The hardness values were determined by taking the average of 10 successful measurements.

In accordance with the inter-granular corrosion test stated in the ISO 11846 standard, corrosion tests of the alloys were placed in glass cells containing a 30 gr/l NaCl+10ml/l HCl solution at room temperature (20-23°C) at various time intervals. The corrosion tests were evaluated by both of mass loss measurements and electrochemical tests. Each data point for both mass loss measurement and electrochemical test represents the average of three different measurements.

For the mass loss measurement method, samples (15 mm × 10 mm × 6 mm) were immersed in the solution for 24 hours. The samples, which were taken out of the solution at certain intervals during the corrosion ex-

periments, were ultrasonically cleaned in distilled water and alcohol, after which they were weighed using a 0.1 mg-sensitive electronic scale. At the same time, the pH, the temperature, and the electrical conductivity of the corrosion solution were measured. The normalised mass loss values of the investigated alloys were calculated as g/mm2 by dividing the mass loss of the each sample by their initial total surface area. Finally, the cross section images of the corroded samples were examined using an optical microscope in order to determine the morphology of the developed corrosion, after applying the conventional metallographic preparation procedure.

For the electrochemical corrosion tests, samples were attached to a copper wire and embedded into an epoxy resin holder, to allow an open surface area of 0.19 cm^2. Potentiodynamic polarisation curves were obtained using a Gamry PC+/300 mA potentiostat/galvanostat, controlled by a computer with DC105 corrosion analysis software. The potentiodynamic polarisation curves were generated by sweeping the potential from a cathode direction to an anode direction, at a scan rate of 1 mV/s, starting from -500 mV up to +500 mV. Corrosion potentials (E_{corr}) and corrosion current densities (i_{corr}) were calculated using a Tafel type fit in the software.

3. Results and discussion

3.1. The Microstructure and the micro-hardness of the alloys

Fig. 1 illustrates the SEM images of the investigated alloys. The microstructure images illustrated in Fig. 1 show the dark globular grey-coloured phase and rod-shaped phases formed at the grain boundaries. EDS analysis results taken from the dark non-shaped grey-coloured phases (Fig. 1, Phase No. 2) proved that this phase was rich in Al, Mg, and Si. According to EDS analyses and studies in literature [17,18], the non-shaped dark grey-coloured phase is Mg_2Si. The EDS results taken from the rod-shaped phase, formed in the microstructure of the Ti-added AA 6063 alloys, showed that this phase is rich in terms of Ti; in accordance with studies in literature [19,20], this phase is thought to be Al_3Ti.

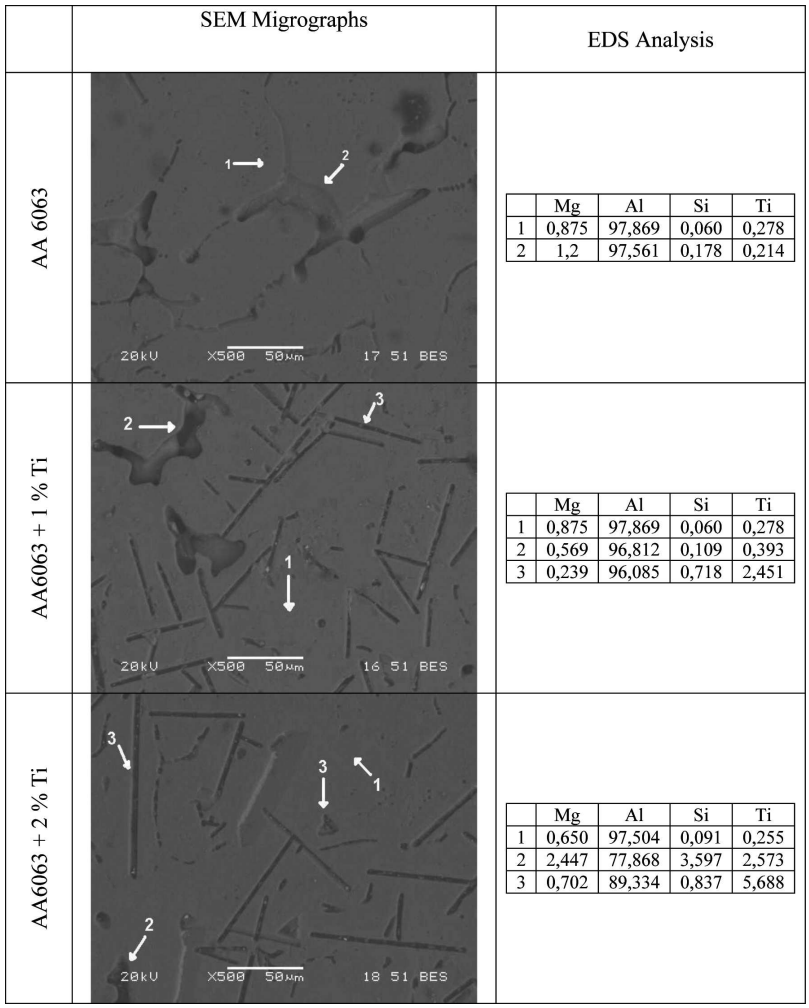

	Mg	Al	Si	Ti
1	0,875	97,869	0,060	0,278
2	1,2	97,561	0,178	0,214

	Mg	Al	Si	Ti
1	0,875	97,869	0,060	0,278
2	0,569	96,812	0,109	0,393
3	0,239	96,085	0,718	2,451

	Mg	Al	Si	Ti
1	0,650	97,504	0,091	0,255
2	2,447	77,868	3,597	2,573
3	0,702	89,334	0,837	5,688

Fig. 1. SEM Micrographs and EDS analysis taken from the microstructure of the alloys heat treated peak-aged conditions at 150°C

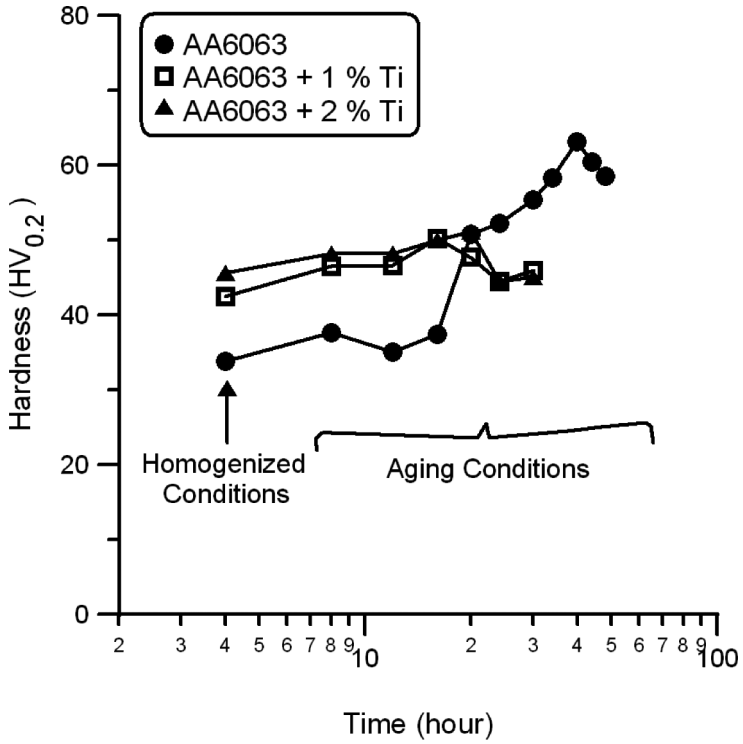

Fig. 2. Matrix hardness of the investigated alloys

Fig. 1 illustrates that as the Ti content of the alloy increases, the Al_3Ti phase tends to elongate and become plated. Fig. 1 also illustrates that as the quantity of added Ti content increases, the Al_3Ti phase becomes rich in terms of Si. This means that when the amount of Si in the matrix decreases and formation of the Mg_2Si phase is restricted.

Fig. 2 illustrates the variation in the hardness of the homogenised and aged alloys for 48 hours at 150°C against the aging time. After adding 2% Ti into the alloy, the hardness of the homogenised alloy increased by 35%. It can be said that the increase observed in the hardness of the Ti-added AA 6063 alloy, after homogenising, is based on the increase in the amount of the Al_3Ti phase and its coarsening (Fig. 1). The change in the peak-aged hardness of the aged Ti free alloys, against the aged time (Fig. 2), post homogenising heat treatment, is 86%, the hardness of Ti-added alloys is low. While the hardness of the alloy containing 1% Ti increased by 19%, the hardness of the alloy containing 2% Ti increased around 10%.

The hardening phase, which enables the increase in hardness after aging heat treatment, is Mg_2Si in Al-Mg-Si alloys [17,21-24]. The significant reason why hardness does not increase in Ti-added alloys, after applying aging heat treatment, under peak aging conditions, is the fact that the amount of Mg_2Si is low, as stated previously. In addition, the Al_3Ti intermetallics, formed in the structure, affected the aging parameters (peak aging time, etc.). While the Ti-free AA 6063 alloys reached a maximum hardness after a 40-hour aging process, the Ti-added alloys reached a maximum hardness after a 20-hour aging process.

3.2. Corrosion behaviour

The mass loss against time and the potential curves for the homogenised and aged alloys in the solution of 30 gr/l sodium chloride and 10 ml/l hydrochloric acid in de-ionized water exposed to atmospheric air are illustrated in Fig. 3 and Fig. 4 respectively. The mass loss vs. time graphs has two regions; the first six hours are the initial state period, and the period after six hours is the steady-state period. While mass loss progresses rapidly during the initial state period, the mass loss rate reaches a steady value in the steady-state period. The mass loss rate is the gradient of the lines in the steady-state period illustrated in Fig. 3. In addition to this conclusion, Fig. 3 illustrates that the mass loss in homogenised alloys is higher than that in aged alloys. Among the investigated alloys, Ti-free AA 6063 alloys displayed higher mass loss, while the mass loss for the AA 6063 alloys containing 1% Ti is lower than the other alloys.

According to the potential-current density graphs (referred to as polarisation curves from herein) of the homogenised and aged alloys, the corrosion current density (i_{corr}) changes with the alloy types investigated, while the corrosion potential (E_{corr}) becomes relatively con-

stant at 760 volt. In line with mass loss test results, i_{corr} values indicate a faster corrosion rate for Ti-free, and 2 % Ti-added AA6063 alloys were higher than AA6063 alloys containing 1% Ti.

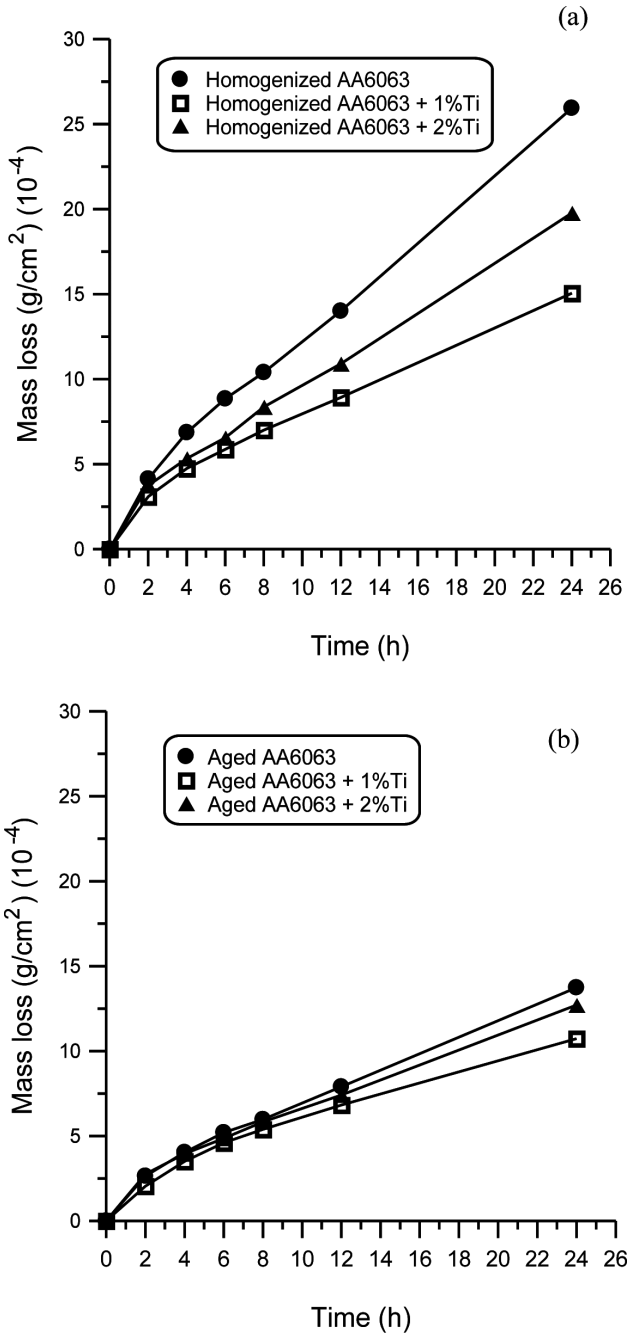

Fig. 3. The mass loss values of the (a) homogenized and (b) aged alloys as a function of the time

Fig. 5 illustrates the change in mass loss rate and corrosion current density values, extracted respectively from Fig. 3 and Fig. 4, for Ti-added alloys investigated. Adding 1% Ti to the alloy decreased both the mass loss rate and the corrosion current density, whereas both properties increased when more than 1% Ti was added. Reduction rate of hydrojen ions increasing with increasing corrosion(mass loss rate and corrosion current density). As a result, hydrogen ions are used in the adjacent region of the electrode surface, and the pH value of the solution increases. With the increase in corrosion, as a result of the investigated alloys dissolving in ionised form, the conductivity of the solution increased. The pH (Fig. 6) and the conductivity (Fig. 7) of the used solution in this study were measured before and after the corrosion experiment. Conductivity and pH in the corrosion solution of the AA 6063+1% Ti alloy was lower than the others. However, in a study conducted by Ralston et al. [25] they determined that the i_{corr} values decreased as low as a certain pH, after which the pH increased together with the increase in the i_{corr} values, in accordance with this study.

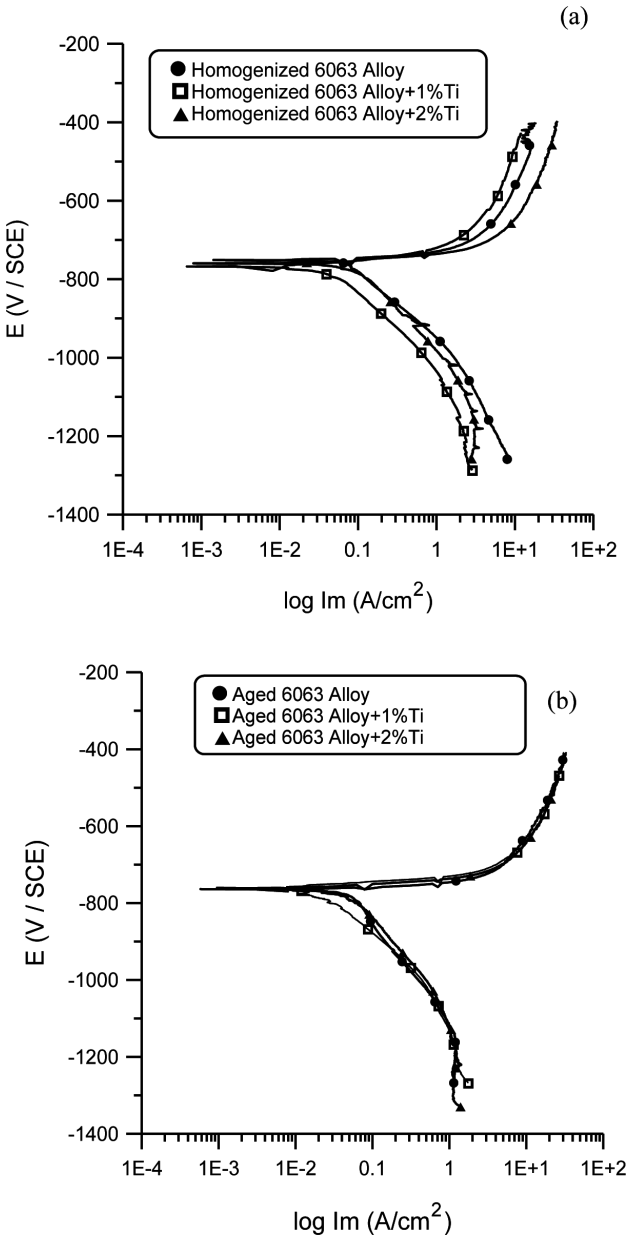

Fig. 4. The potential values for the (a) homogenized and (b) aged alloys as a function of the current density

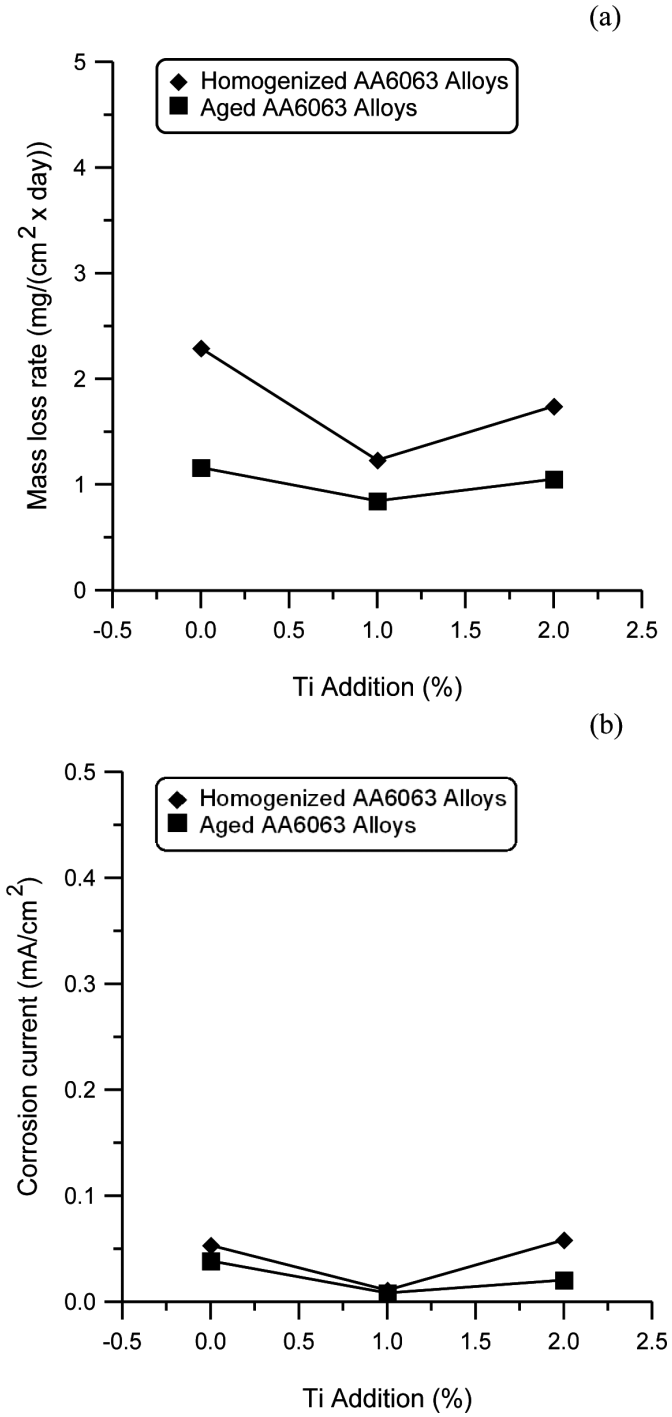

Fig. 5. a) Mass loss rate and b) Corrosion current density of the investigated alloys as a function of the Ti addition

The Al_3Ti intermetallic, formed in the microstructure with the addition of Ti to the AA6063 alloy, is nobler in terms of corrosion than the other microstructure compounds (such as matrix and the Mg_2Si intermetallic). The Al_3Ti intermetallic improves corrosion behaviour because it is in fine needle form, and the addition of 1% Ti restricts the formation of Mg_2Si in the structure [11,12]. Since adding a higher amount of Ti leads to an increase in the number of Al_3Ti phases, the corrosion rate is also expected to increase due to galvanic coupling [26]. Al_3Ti is likely to exhibit cathodic behaviour, relative to the matrix, resulting in more dissolution [11, 18, 27]. Based on galvanic corrosion principles [28], a small cathode (intermetallics) in relation to the size of the anode (Al matrix) results in a reduced galvanic corrosion.

The reason why corrosion decreases when aging heat treatment is applied to the investigated alloys can be due to the refining intermetallics (Al_3Ti and Mg_2Si) and their homogenous distribution in precipitation form during aging heat treatment. In conclusion, a decrease in the cathode surface area occurs during aging heat treatment, which triggers a decrease in galvanic corrosion.

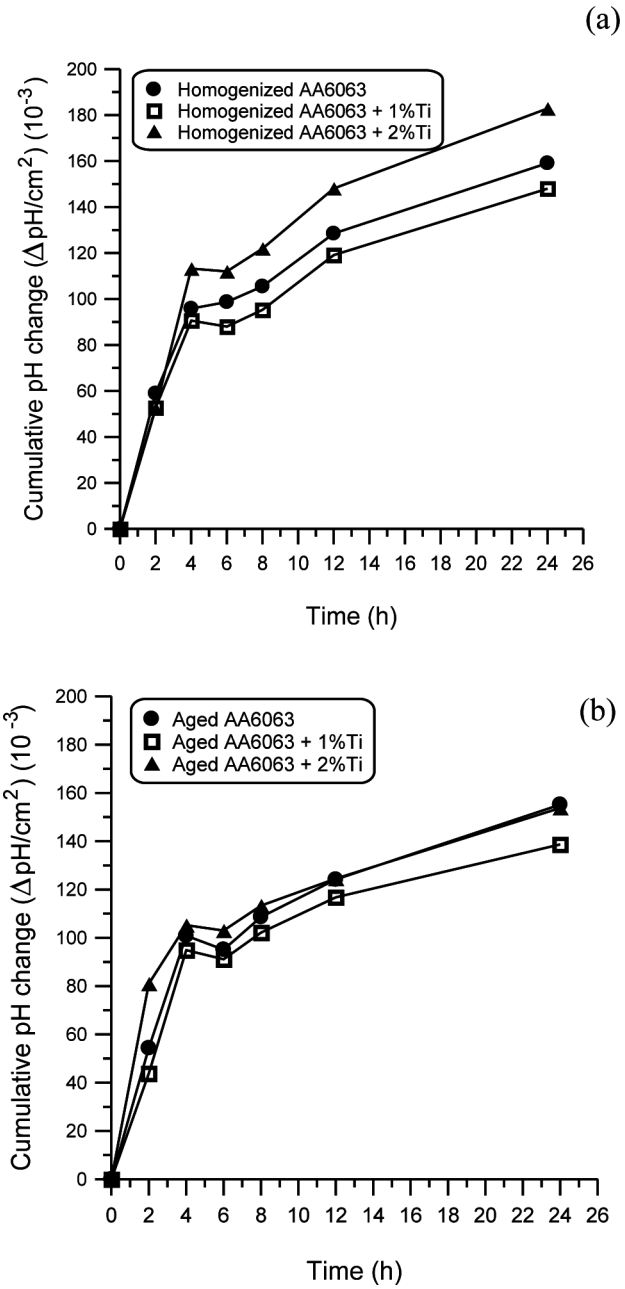

Fig. 6. The cumulative PH change for the (a) homogenized and (b) aged alloys as a function of time

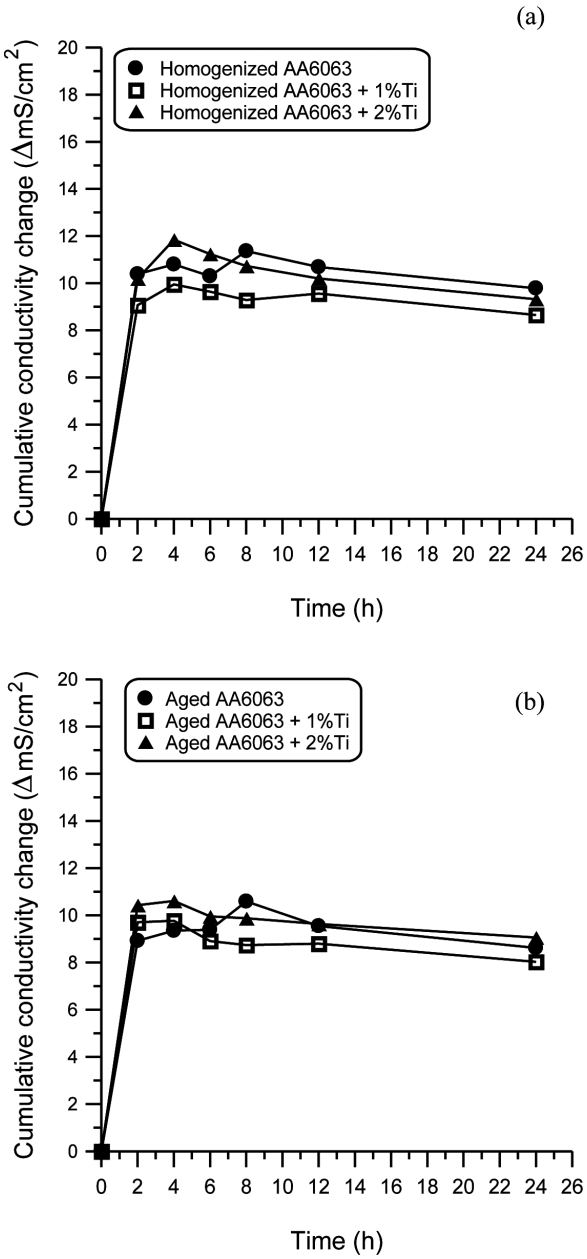

Fig. 7. The cumulative conductivity change for the (a) homogenized and (b) aged alloys as a function of time

Fig. 8 illustrates the optic microscope images taken from the cross section of the alloys, prepared after corrosion experiments. Corrosion progressed in the form of pitting. Pitting in 2% Ti-added alloys nucleates and proceeds around the Al_3Ti intermetallic. In accordance with the results stated above, aging heat treatment slowed down corrosion significantly. In Ti-free alloys, corrosion was caused by pitting and progressed between grains. Literature [5-9,14,15] states that Al alloys containing precipitate are susceptive to inter-granular corrosion. The cross section image of the alloy, taken after the experiment, illustrates cracks that start from the surface and progress inwards. In Ti-free AA 6063 alloys, cracks progressing inwards from the surface decreased with aging heat treatment.

Previous corrosion studies conducted on Al alloys [2,4-15] have focused on the corrosion susceptibly in corrosion solution e.g. Sodium chloride. Researchers [7-9,13] reported that pits initiate around secondary particles within the matrix. However, Kiourtsidis and Skalianos [29] explained that the progress of corrosion using two anodic reactions; namely corrosion of the matrix adjacent to intermetallic regions, and pitting of dendrite cores, instead of galvanic corrosion, developed between the intermetallic and matrix.

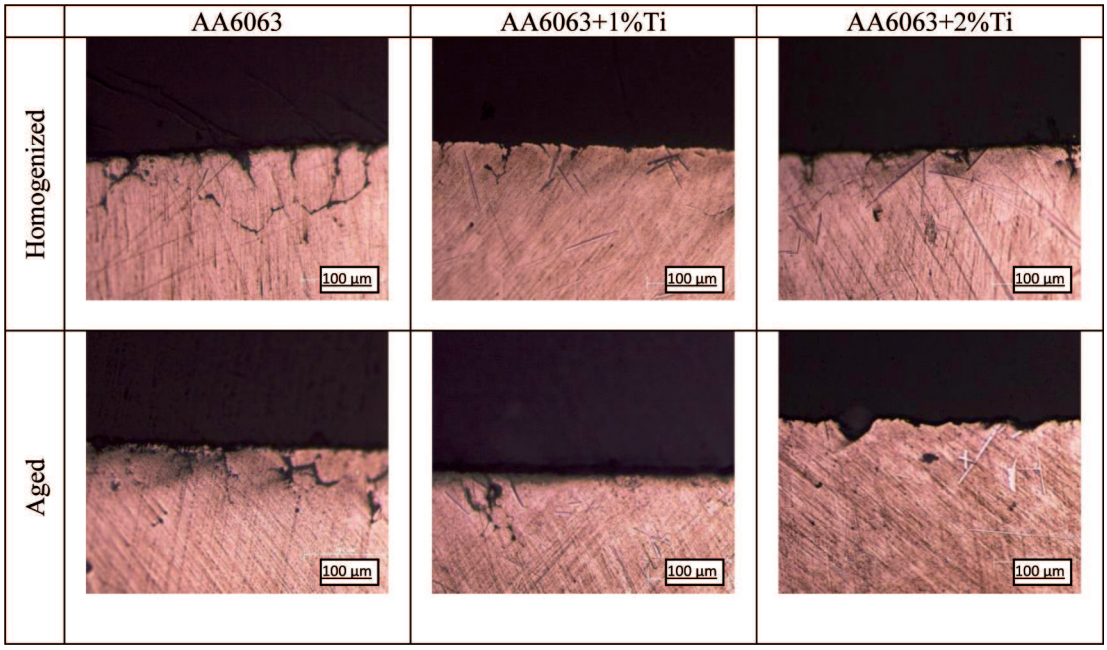

Fig. 8. LOM micrographs showing cross section of homogenized and aged alloys

4. Conclusion

Stated below are the general conclusions obtained from this study, which investigated the effects that adding Ti and applying aging heat treatment to AA6063 cast alloys had on their corrosion properties.

1. Non-shaped dark grey-coloured phases and rod-shaped phases, formed at the grain boundaries, are seen in the microstructure images of the investigated alloys. According to the EDS results the non-shaped dark grey-coloured phase is the Mg_2Si. The rod-shaped phase formed in the microstructure of Ti-added AA 6063 alloys was identified as Al_3Ti. It was identified that as the amount of Ti content increased the Al_3Ti elongated and become plated.
2. The hardness of the alloys subjected to the homogenising heat treatment increased with the increase in Ti content. However, while Ti-free alloys reached higher peak aged hardness over a longer period, Ti-added alloys reached lower peak aged hardness over a shorter period.
3. The results of the corrosion tests proved that the rate of corrosion decreased in the alloys containing less than 1% Ti, and the rate of corrosion increased in alloys containing more than 1% Ti and Ti free, in both homogenised and aged conditions. Another observation was that aging heat treatment improved the corrosion resistance.

REFERENCES

[1] A. Meyveci, İ. Karacan, U. Çalıgülü, H. Durmuş, Pin-on-disc characterization of 2xxx and 6xxx aluminium alloys aged by precipitation age hardening. Journal of Alloys and Compounds **491**, 278-283 (2010).

[2] W. Weiwei, H. Jianmin, L. Weijing, W. Jinhua, Study of rare earth element effect on microstructures and mechanical properties of an Al-Cu-Mg-Si cast alloy. Rare Metals **25**, 129-132 (2006).

[3] A.S. Anasyida, A.R. Daud, M.J. Ghazali, Dry sliding wear behaviour of Al-12Si-4Mg alloy with cerium addition. Materials and Design **31**, 365 (2010).

[4] A.K. Bhattamishra, K. Lal, Microstructural studies on the effect of Si and Cr on the intergranular corrosion in Al-Mg-Si alloys, Materials Design 18, 25-28 (1997).

[5] T. Ramgopal, P.I. Gouma, G.S. Frankel, Role of grain boundary precipitates and SDZ on the intergranular corrosion of aluminum alloy AA7150. Corrosion Science Section **58**, 687-697 (2002).

[6] P. Leblanc, G.S. Frankel, A study of corrosion and pitting initiation of AA2024-T3 using atomic force microscopy. Journal of Electrochemical Society 149, 239-247 (2002).

[7] W. Zhang, G.S. Frankel, Localized corrosion growth kinetics in AA2024 alloys. Journal of Electrochemical Society **149**, 510-519 (2002).

[8] Y. Baek, G.S. Frankel, Electrochemical quartz crystal microbalance study of corrosion of phases in AA2024. Journal of Electrochemical Society **150**, 1-9 (2002).

[9] W. Zhang, G.S. Frankel, Transitions between pitting and intergranular corrosion in AA2024. Electrochımıca Acta **48**, 1193-1210 (2003).

[10] Q. Meng, G.S. Frankel, Effect of Cu content on corrosion behavior of 7xxx series aluminum alloys. Journal of Electrochemical Society **151**, 271-283 (2004).

[11] N. Birbilis, R.G. Buchheit, Corrosion damage accumulation on high strength aluminum alloys: Some advances in understanding the role of intermetallics. Corrosion and Materials **29**, 4-10 (2004).

[12] N. Birbilis, R.G. Buchheit, Electrochemical characteristic of intermetallic phases in Al alloys. Journal of Electrochemical Society 152, 140-151 (2004).

[13] H. Santos, F. Reis, C. Kunioshi, J. Rossi, I. Costa, Corrosion performance of Al-Si-Cu hypereutectic alloys in a synthetic condensed automotive solution. Materials Research **8**, 155-159 (2005).

[14] G. Svenningsen, M.G. Larsen, J.C. Walmsley, J.H. Nordlien, K. Nişancıoğlu, Effect of artifical aging on intergranular corrosion of extruded AlMgSi alloy with small Cu content. Corrosion Science 48, 1528-1543 (2006).

[15] T. Huang, G.S. Frankel, Influence of grain structure on anisotropic localised corrosion kinetics of AA7xxx-T6 alloys. Corrosion Engineering Science and Technology 41, 192-199 (2006).

[16] L.A. Dobrzanski, K. Labisz, A. Olsen, Microstructure and mechanical properties of the Al-Ti alloy with calcium addition. Journal of Achievements in Materials and Manufacturing Engineering **26**, 183-188 (2008).

[17] M. Gavgali, Y. Totik, R. Sadeler, The effect of artificial aging on wear properties of AA 6063 alloy. Materials Letters **57**, 3713-3721 (2003).

[18] H. Ahlatci, A. Durmaz, A. Balta, M. Acarer, E. Candan, Effect of Ti on the corrosion behaviour of in-situ Mg_2Si particle reinforced Al-12Si-20Mg-XTi alloys. Materials Science Forum 636, 511-516 (2010).

[19] N. Saheb, T. Laoui, A.R. Dauda, M. Harun, S. Radimana, R. Yahaya, Influence of Ti addition on wear properties of Al–Si eutectic alloys. Wear **249**, 656-662 (2001).

[20] K. Das, L.K. Narnaware, A study of microstructure and tribological behaviour of Al-4.5% Cu /Al3Ti Composites. Materials Characterization **60**, 808-816 (2009).

[21] R.A. Siddiqui, H.A. Abdullah, Influence of aging parameters on the mechanical properties of 6063 aluminium alloy. Journal of Materials Processing Technology **102**, 234-240 (2000).

[22] M. Gavgali, Y. Totik, R. Sadeler, I. Kaymaz, Improvements of fatigue behavior in 2014 Al alloy by solution heat treating and age-hardening. Wear **236**, 144-152 (2004).

[23] H. Kaçar, E. Atik, C. Meriç, The effect of precipitation-hardening conditions on wear behaviors at 2024 aluminium wrought alloy. Wear **236**, 144-152 (2003).

[24] D.G. Altenpohl, Aluminum technology, applications and environment a profile of a modern metal. 6th ed. TMS (1998).

[25] K.D. Ralston, S. Chrisanti, T.L. Young, R.G. Buchheita, Corrosion inhibition of aluminum alloy 2024-T3 by aqueous vanadium species. Journal of The Electrochemical Society **155**, 350-359 (2008).

[26] M. Cavanaugh, N. Birbilis, R.G. Buchheit, F. Bovard, Investigating localized corrosion susceptibility arising from Sc containing intermetallic Al_3Sc in high strength Al-alloys. Scripta Materialia 56, 995-998 (2007).

[27] N. Birbilis, R.G. Buchheit, An experimental survey of electrochemical characteristics for intermetallic phases in aluminum alloys. Journal of the Electrochemical Society **152**, 140-146 (2005).

[28] M. Anik, P. Avci, A. Tanriverdi, İ. Çelikyurek, B. Baksan, R. Gurler, Effect of the eutectic phase mixture on the anodic behavior of alloy AZ91. Mater. Design 27, 347-355 (2006).

[29] G. Kiourtsidis, S.M. Stolianos, Corrosion behaviour of squeze-cast silicon carbide -2024 composites in aerated 3.5% sodium chloride. Mater. Sci. Eng. **A 248**, 165-172 (1998).

Received: 20 November 2011.